Three-dimensional surface current loops in broadband responsive negative refractive metamaterial with isotropy*

He Xun-Jun(贺训军)†, Wang Yue(王 玥), Mei Jin-Shuo(梅金硕), Gui Tai-Long(桂太龙), and Yin Jing-Hua(殷景华)

School of Applied Sciences, Harbin University of Science and Technology, Harbin 150080*, China*

(Received 9 June 2011; revised manuscript received 18 October 2011)

We propose a bulk negative refractive index (NRI) metamaterial composed of periodic array of tightly coupled metallic cross-pairs printed on the six sides of a cube for applications of superlenses. The structural characteristics of the three-dimensional (3D) metamaterial consist in the high symmetry and the superposition of metallic cross-pairs, which can increase the magnetic inductive coupling between adjacent cross-pairs and realize a broadband and isotropic NRI. The proposed 3D structure is simulated using the CST Microwave Studio 2006 to verify the design validity. The simulation results show that the proposed structure can not only realize simultaneously an electric and magnetic response to an incident electromagnetic (EM) wave, but also exhibit a broadband NRI whose relative bandwidth can reach up to 56.7%. In addition, the NRI band is insensitive to the polarization and the incident angle of the incident EM wave. Therefore, the proposed metamaterial is a good candidate material as three-dimensional broadband isotropic NRI metamaterial.

Keywords: surface current loops, broadband, isotropy, metamaterial

PACS: 41.20.Jb, 42.25.Bs, 73.20.Mf, 77.22.Ch **DOI:** 10.1088/1674-1056/21/4/044101

1. Introduction

The negative refractive index (NRI) metamaterials are artificially composite structures exhibiting simultaneously a negative permeability and negative permittivity over a common frequency range. Such metamaterials have recently attracted considerable attention and obtained rapid development due to their unique electromagnetic properties.[1] Currently, a variety of NRI metamaterials have been designed and fabricated,[2−4] based on the analogous principle combining periodic split ring resonator (SRR)/Wire.[5] However, their negative refractions are achieved only when a fixed polarization EM wave parallelly propagates the sample surfaces, due to anisotropy structures. This results in high anisotropy and strong polarization dependence, which will seriously affect and restrict their practical applications, especially when isotropic applications are targeted for obtaining superlenses.[6] Therefore, the realization of a polarization-independent and isotropic NRI metamaterial is a hot subject of the NRI metamaterial research.

It is well known that the NRI metamaterials mentioned above are mostly two-dimensional structures, which are based on a planar concept.[7,8] Comparatively, the three-dimensional (3D) structure easily realizes the isotropy and polarization independence, due to the high symmetry of the unit cell.[9,10] Currently, the realization of the 3D NRI metamaterials has two modes. One is the distributed structures based on transmission lines or lumped-elements,[11,12] and the other is the bulk medium structures based on the extension of two-dimensional (2D) NRI structure[13−16] or resonant dielectric spheres.[17,18] Moreover, both methods can realize isotropy and polarization independence. But, the NRI characteristics are obtained only in the given frequency band and moreover the bandwidths are rather narrow,[14,19] which seriously restricts their practical applications.

In this paper, we propose a new type of 3D bulk metamaterial composed of periodic array of tightly

*Project supported by the National Natural Science Foundation of China (Grant No. 51005001), the National Science Foundation for Post-doctoral Scientists in China (Grant No. 20090450226), the Research Foundation of Education Bureau of Heilongjiang Province, China (Grant No. 11551098), and the Youth Foundation of Harbin University of Science and Technology, China (Grant No. 2009YF024).

†Corresponding author. E-mail: hexunjun@yahoo.com.cn

© 2012 Chinese Physical Society and IOP Publishing Ltd

coupled metallic cross-pairs printed on the six sides of a cube. The special characteristics of the 3D metamaterial consist in high symmetry and superposition of metallic cross-pairs, thus, it can not only realize isotropy, but also exhibit strong magnetic inductive coupling between adjacent cross-pairs, consequently realizing a broad isotropic metamaterial. In order to verify the validity of the proposed design and better understand the physical mechanism of broadband NRI, the scattering parameters and field distribution of the proposed 3D metamaterial structure in the case of different incidence conditions are analysed using the CST Microwave Studio 2006, and the corresponding effective parameters (permeability, permittivity, and refractive index) of the structure are retrieved from scattering parameters obtained by simulations based on the retrieved program. The simulation results demonstrate that this 3D structure not only exhibits polarization independence and isotropy, but also obtains a broadband NRI region, in which the ratio of the negative bandwidth to the central frequency of the NRI is up to 56.7%.

2. Structure design and simulation

To realize a broadband and isotropic NRI metamaterial, we design a new type of 3D bulk metamaterial composed of tightly coupled metallic cross-pairs printed on the six sides of a cube, which is periodically infinite in the x–y plane as shown in Fig. 1. The advantage of this unit cell is that it is able to realize the high symmetry and superposition of metallic cross-pairs. As in earlier NRI structure,[5] the bars of our metallic cross-pairs are analogous to small electrical dipoles, which are responsible for an electric resonance, while the adjacent cross-pairs can produce an equivalent current loop when the structure is excited by the EM wave, thus exhibiting a magnetic resonance. If both magnetic and electric resonances simultaneously occur in the same frequency band by adjusting structural parameters, the structure can realize an effective NRI performance. Owing to the high symmetric structure, the structure can provide an isotropic response to any linearly polarized incident wave. In addition, the structure can also be considered as the superposition of cell-to-cell to form a 3D surface current, which can produce a strong magnet-inductive coupling between neighbouring cross-pairs, resulting in a broadband NRI behaviour.[20−22] Therefore, the proposed metamaterial can exhibit a broadband and isotropic NRI characteristic.

In order to verify our speculation, the proposed 3D metamaterial structure is numerically analysed using CST Microwave Studio 2006 by imposing the special boundary conditions, where the periodic boundaries correspond to the $\pm x$ sides and $\pm y$ sides of a cube unit cell respectively, while the open boundaries correspond to $\pm z$ sides of two cubic unit cells, respectively. Thus, the simulated structure can be considered as an infinitely wide metamaterial slab with a thickness of two unit cells. To illustrate the incident state of EM wave in simulation, figure 1(a) shows the incidence angle and the polarization angle of the incident plane wave, where $\boldsymbol{k}$ is the oblique incident plane wave vector with the incidence angle $\theta_{\rm i}$ with respect to the z direction, and polarization angle $\phi_{\rm i}$ which is the angle between the projection of $\boldsymbol{k}$ in the x–y plane and the x direction. While, figure 1(b) shows the unit cell of the structure, where the metallic cross-pairs are made of copper with conductivity $\sigma = 5.8 \times 10^7$ S·m^{-1} and thickness $t = 0.035$ mm, and etched on an FR-4 dielectric cube with dielectric constant $\varepsilon_{\rm r} = 4.9$ and loss tangent $\mathrm{tg}\,\delta = 0.025$. The length of the cube edge is $a = 3$ mm, while the width w and length l of cross-pairs are 0.6 mm and 2.8 mm, respectively.

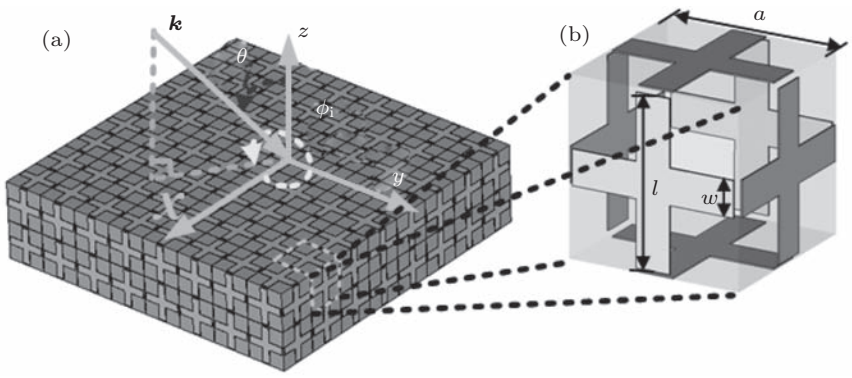


Fig. 1. Proposed 3D bulk metamaterial: (a) schematic diagram and (b) unit cell of structure.

To better understand the NRI physical mechanism of the proposed 3D metamaterial structure, we firstly calculate the field and the surface current distributions of the unit cell structure under normal incidence at $\theta_{\rm i} = 0$ and $\phi_{\rm i} = 0$. Figures 2 and 3 show the calculated results of field distributions at 12 GHz. Figures 2(a) and 2(b) show the general solid view and perspective view of electric field distributions, respectively. As can be seen clearly from Figs. 2(a) and 2(b), the front and the back adjacent cross-pairs carry electrical charges with opposite signs, which are analogous to small electrical dipoles. Moreover, the electric field between the ends of the front and the back adjacent cross-pairs is very strong. These results indicate that there is a strong electric resonance, thus a negative effective permittivity is expected in the negative resonance frequency range.

Figures 3(a) and 3(b) show the perspective view and sectional view in x–y plane of surface current distributions for the same unit cell, respectively. As shown in Figs. 3(a) and 3(b), the surface currents on the front cross-pairs are antiparallel to that on the back adjacent cross-pairs everywhere, moreover the surface currents on both side cross-pairs are also the same. Thus, the antiparallel surface currents on the cross-pairs above four planes combining with the displacement currents of the substrate form an equivalent current loop, which can be represented as equivalent magnetic dipole moment, while the arrows in Fig. 3(b) represent the directions of the current loop. This magnetic moment is responsible for the artificial magnetism of the structure, and therefore such a resonance is referred to as a magnetic resonance.

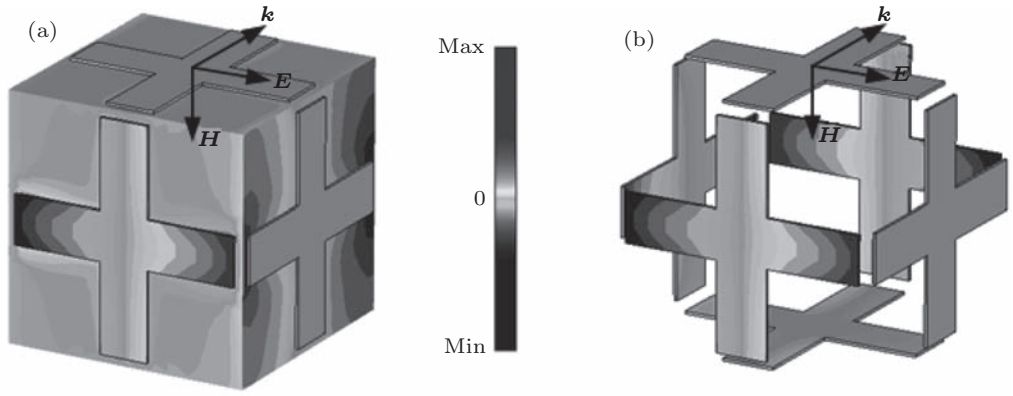


Fig. 2. Electric field distributions of unit cell structure under normal incidence at $\theta_{\rm i} = 0$, $\phi_{\rm i} = 0$, and 12 GHz: (a) general solid view, and (b) perspective view.

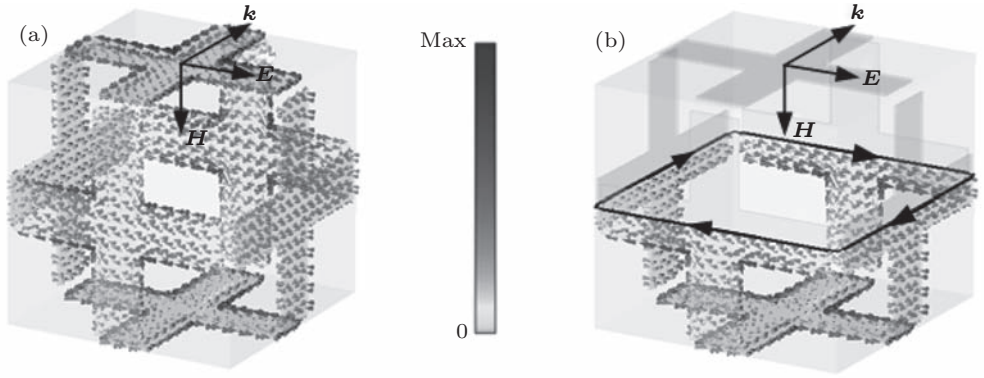


Fig. 3. Surface current distributions of unit cell structure under normal incidence at $\theta_{\rm i} = 0$, $\phi_{\rm i} = 0$, and 12 GHz: (a) perspective view and (b) sectional view.

It is well known that the electric and the magnetic dipole moments are thought of as the basic alphabet for constructing NRI metamaterial.[23] In the unit cell structure of our 3D metamatrial, the strong electric field between the ends of the front and the back adjacent cross-pairs can be equivalent to an elec-

tric dipole, exhibiting an electric resonance. While, the current loop formed by combining surface currents on the front and the back cross-pairs as well as both side cross-pairs with displacement currents of the substrate can be equivalent to a magnetic dipole, exhibiting a magnetic resonance. Moreover, the electric and the magnetic resonances can simultaneously occur in the same frequency band by adjusting structural parameters. Therefore, the 3D metamaterial structure based on such a unit cell structure is expected to be a candidate of 3D NRI metamaterial.

3. NRI property of 3D metamaterial structure

To analyse the NRI property of the proposed 3D metamaterial structure, we calculate the scattering parameters of the proposed 3D metamaterial structure under normal incidence at $\theta_{\rm i} = 0$ and $\phi_{\rm i} = 0$. Figure 4 shows the magnitudes and the phase spectra of the calculated scattering parameters. The calculated magnitude of scattering parameter S_{11} (reflection) presented in Fig. 4(a) shows clearly two resonance dips, the first one is at 8.3 GHz and the second one is at 15.1 GHz. Moreover, the reflection magnitude shows a wider dip around 8.3 GHz than around 15.1 GHz, where the scattering parameter S_{21} (transmission) has a maximum value and quite a broad pass-band. We also note in Fig. 4(b) that a change in sign occurs abruptly for the transmission phase at the first resonance dip (8.3 GHz), subsequently the transmission phase reduces monotonically with frequency increasing. In general, the phase factor of the propagating EM wave is defined as the $\exp(-\,{\rm i}\,n\boldsymbol{kr})$, with $\boldsymbol{k}$ being the incident wave vector and $\boldsymbol{r}$ the propagation distance. Thus, the transmission phase is defined as the $\Phi = -n\boldsymbol{kr}$. In Fig. 4(b), we obtain the positive transmission phase, which indicates that the EM wave must propagate inside a material with negative index n, due to both $\boldsymbol{k} > 0$ and $\boldsymbol{r} > 0$.[24] Therefore, this result further demonstrates that the realization of the NRI characteristic is possible for our proposed 3D structure.

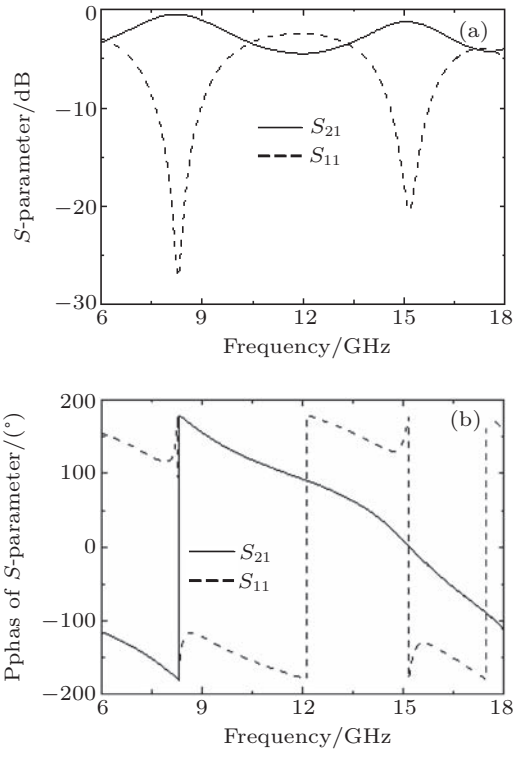


Fig. 4. Calculated magnitude (a) and phase (b) spectra of the transmission and reflection of the proposed 3D metamaterial under normal incidence at $\theta_{\rm i} = 0$ and $\phi_{\rm i} = 0$.

In order to further analyse the NRI characteristic, based on the calculated scattering parameters, the constitutive parameters of the proposed structure, which mean effective permittivity ε, permeability μ, and refractive index n, can be extracted by the retrieval procedures proposed in Refs. [25] and [26]. The four equations listed below are the main formulas to calculate the constitutive parameters, respectively:

$$z = \pm\sqrt{[(1+S_{11})^2 - S_{21}^2]/[(1-S_{11})^2 - S_{21}^2]}, \quad (1)$$

$$\exp({\rm i}\,nk_0d) = X \pm {\rm i}\,\sqrt{[(1-X)^2}, \quad (2)$$

$$\varepsilon = n/z, \quad (3)$$

$$\mu = nz, \quad (4)$$

where $X = (1 - S_{11}^2 + S_{21}^2)/(2S_{21})$, k_0 denotes the wave number of the incident wave in free space, and d represents the thickness of the slab sample.

Figure 5 shows the extracted effective permittivity ε, permeability μ, and refractive index n of the proposed 3D metamaterial under normal incidence at $\theta_{\rm i} = 0°$ and $\phi_{\rm i} = 0°$. In Figs. 5(a) and 5(b), the proposed 3D metamaterial structure exhibits the same magnetic and electric resonant characteristics around the first reflection resonance dip in Fig. 4(a), due to high symmetry of the unit cell structure. Moreover, the real parts of effective permeability and permittivity each present a sudden jump from positive to negative in the vicinity of the first reflection resonance. This can be explained as the special propagating performance of the EM wave in the structure, where the transmission phase abruptly changes sign from negative to positive as shown in Fig. 4(b).[24] Then, the real parts of effective permittivity and permeability

each undergo a negative value region. Finally, we can notice that the zero values for the ε and μ responses are very close to the second reflective resonance dip in Fig. 4(a), where a small transmission band is observed in Fig. 4(a). Thus, the real parts of effective permittivity and permeability can exhibit simultaneously negative values in a frequency range from 8.24 GHz to 14.76 GHz, which indicates that there exists a negative refractive index n in this region. As shown in Fig. 5(c), an NRI band is achieved in the above double negative region. Moreover, the NRI bandwidth can attain up to 6.52 GHz and the relative bandwidth can be up to 56.7%, which is superior to the currently reported results.[14] Therefore, the proposed 3D metamaterial can be regarded as a broadband negative refractive metamaterial.

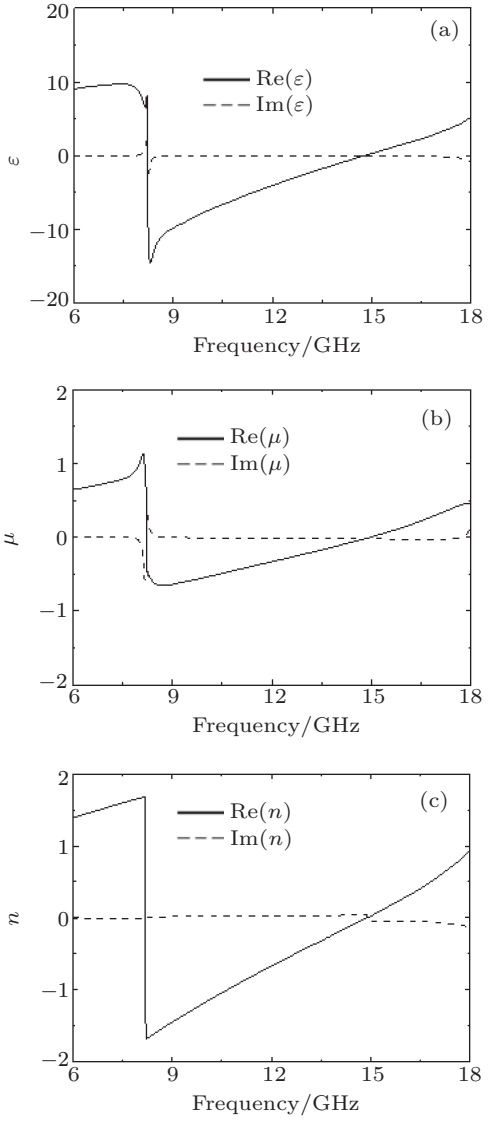


Fig. 5. Magnitudes of retrieved effective parameters of the proposed 3D metamaterial under normal incidence at $\theta_{\rm i} = 0^\circ$ and $\phi_{\rm i} = 0^\circ$: (a) effective permittivity, (b) effective permeability, and (c) effective refractive index.

To understand the physical mechanism of the above broadband characteristics, we calculate the field and the surface current distributions of the proposed 3D metamaterial structure, and the results are shown in Figs. 6 and 7. We observe in Fig. 6 that the cross-pairs of adjacent cells for the EM wave propagating direction ($\boldsymbol{k}$) carry electric charges with opposite signs and the equivalent capacitance is concentrated on the overlapping sections of cross-pairs as shown in Fig. 6(b), while the ends of neighbouring cross-pairs for the vertically propagating direction ($\boldsymbol{k}$) also carry opposite electric charges, leading to another type of capacitance between neighbouring cells as shown in Fig. 6(d). At the same time, we also note in Fig. 7 that two large current loops resulting from four cross-pairs between adjacent cells exhibit the opposite current directions in the $\boldsymbol{k}$ direction as shown in Fig. 7(b), while exhibiting two large clockwise current loops in the $\boldsymbol{E}$ direction as shown in Fig. 7(d). In addition, the single metallic cross-pair also produces a small counterclockwise current loop as shown in Figs. 7(b) and 7(d). Consequently, the structure produces the 3D surface current loops due to the superposition of cell-to-cell, forming the strong magnet-inductive coupling between neighbouring cross-pairs by capacitance and inductance, finally resulting in a broadband NRI. Therefore, the metametrial behaves as a traveling wave structure by increasing the mutual coupling between cubes as demonstrated in previous results.[22]

To further verify the NRI broadband characteristics of the proposed structure we construct a wedge-shaped prism of the metamaterial to perform a Snell's law refraction experiment by the CST Microwave Studio 2006. The wedge-shaped prism is composed of a unit cell in the z direction, up to 12 unit cells in the y direction and up to 24 unit cells in the x direction respectively, while the refraction interface is characterized by a staircase pattern with a step ratio of 2:1, which represents a wedge with a 26.6° angle, thus resulting in 168 cells as shown in Fig. 8. This configuration has been adopted in many earlier reported NRI experiments, and it can display a direct image of the negative refraction behaviour.[27,28] In simulation, the wedge-shaped prism is positioned between the perfect electric conductor plates, which serve as top and bottom perfect magnetic boundary conditions to form a two-dimensional waveguide, while open boundary con-

ditions are imposed at the $\pm x$ and $\pm y$ sides of the wedge-shaped prism. When the wedge-shaped prism is excited by a TEM wave of a waveguide port located at the front-side boundary of the structure, the EM wave is incident on the first interface of the wedge-shaped prism normally. After it propagates through the wedge, the wave undergoes the refraction at the second interface.

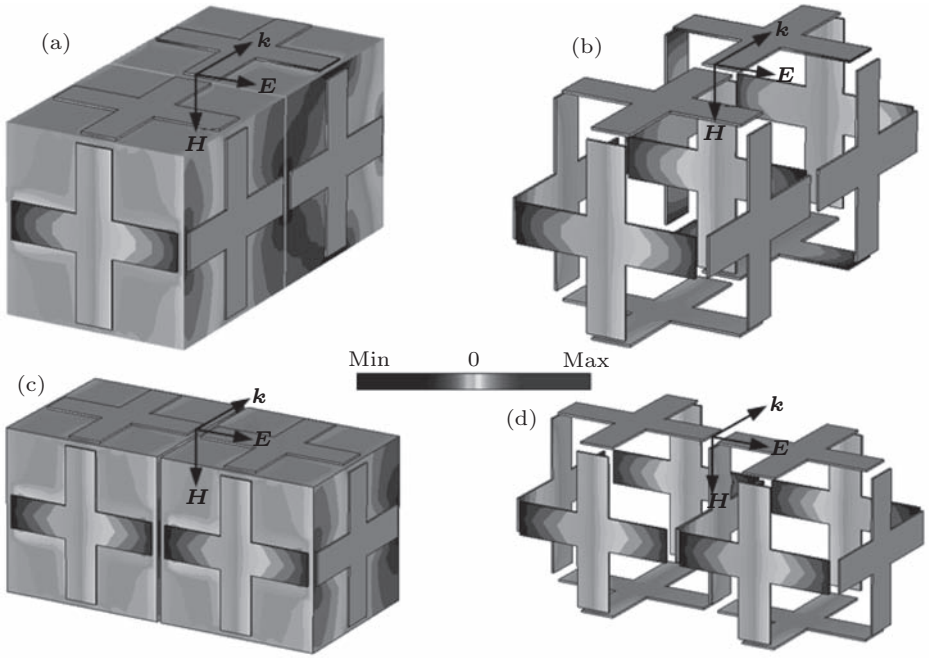


Fig. 6. Electric field distributions of adjacent unit cell structure under normal incidence at $\theta_{\rm i} = 0$, $\phi_{\rm i}$=0, and at 12 GHz: (a) general solid view and (b) perspective view in the $\boldsymbol{k}$ direction, (c) general solid view and (d) perspective view in the $\boldsymbol{E}$ direction.

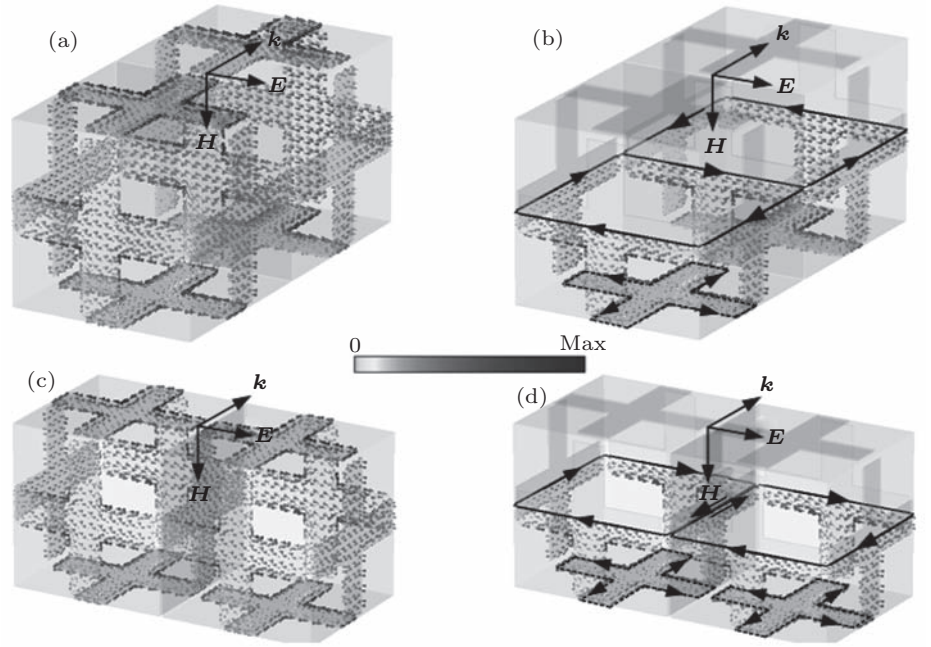


Fig. 7. Surface current distributions of adjacent unit cell structure under normal incidence at $\theta_{\rm i} = 0$, $\phi_{\rm i} = 0$, and 12 GHz: (a) perspective view and (b) sectional view in the $\boldsymbol{k}$ direction, (c) perspective view and (d) sectional view in the $\boldsymbol{E}$ direction.

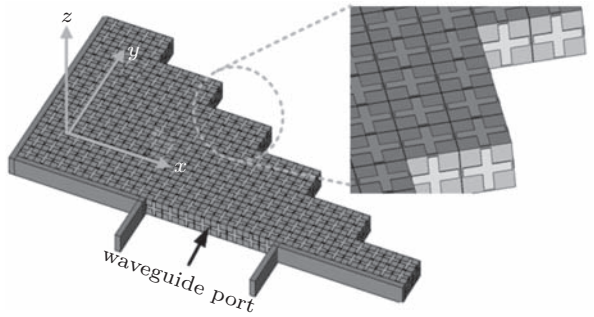


Fig. 8. Rigorous detailed implementation of the metamaterial macrostructure based on proposed 3D unit cell.

The recorded distributions of the electric field at four frequency points in the range of interest are shown in Fig. 9, where the dashed line, solid line, and arrow denote the direction of surface normal, refraction interface, and EM wave respectively. We note in Figs. 9(b) and 9(c) that the negative refractive Gaussian beams are clearly observed at 8.5 GHz and 14.5 GHz falling into the above extracted NRI region. Moreover, they exhibit negative refractive angles of 51.4° and 10.3° at 8.5 GHz and 14.5 GHz respectively and correspondingly calculated refractive indexes are −1.745 and −0.399 based on the extracted refractive angles, which are in good agreement with the retrieval results based on the extracted procedure (−1.661 and −0.12 at 8.5 GHz and 14.5 GHz, respectively). The slight difference between two results is ascribed reasonably to the broadening of the extracted refractive angle. Whereas the refractive wave and the incident wave are on both sides of surface normal at 8 GHz and 15 GHz falling into the above extracted positive refractive index region as shown in Figs. 9(a) and 9(d). Therefore, these results further confirm that the proposed metamaterial has an NRI broadband characteristic.

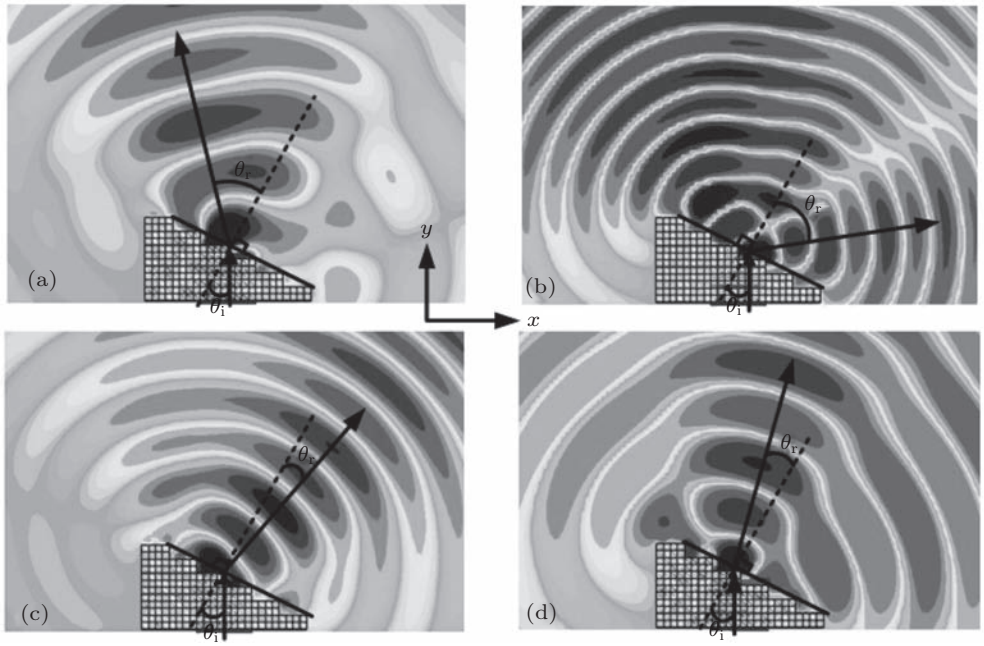


Fig. 9. Electric field distributions of the wedge structure consisting of the proposed 3D unit cell at four different frequencies: (a) 8 GHz, (b) 8.5 GHz, (c) 14.5 GHz, and (d) 15 GHz.

4. Polarization independence and isotropy of metamaterial

To show that the observed negative refraction in our structure is isotropic and polarization-independent for the EM wave incident normally or obliquely as shown in Fig. 1(a), we analyse the influence of incident condition on effective refractive index n. Figure 10 shows the real part Re(n) values of the retrieved effective refractive index under normally incident TE mode plane waves, whose polarizations are rotated by angle $\phi_{\rm i} = 0°$, 20°, 40°, 60°, and 80°, respectively. It is found from Fig. 10 that the real part Re(n) values of the retrieved refractive index do not exhibit any change as the polarization angle of the normally incident TE wave increases. Moreover, there are the same results for the normally incident TM wave (not shown here). These indicate that the proposed

metamaterial structure is independent of the polarization angle of the normally incident EM wave.

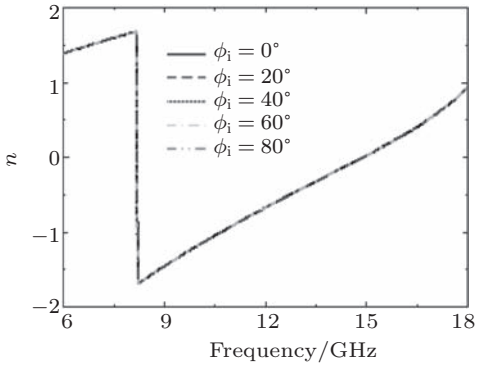


Fig. 10. Curves for Re(n) of retrieved effective refractive index versus frequency for the normally incident TE mode plane wave at different polarization angles.

For the purpose of further achieving a comprehensive response to the obliquely incident TE and TM mode plane waves, we also examine the combined effect of polarization angle and incident angle. Figure 11 shows the real part Re(n) values of the retrieved refractive index of the combined incident and polarization angles of the TE or TM plane wave passing through the proposed metamaterial, where either the polarization angle ϕ_i of TE plane wave increases from 0° to 80° with an interval of 20° when θ_i is set to be 40°, or the incident angle θ_i of the TM plane wave changes from 0° to 80° with an interval of 20° when ϕ_i is set to be 40°. In Fig. 11(a), the real part Re(n) values of the retrieved effective refractive index are nearly independent of the polarization angle as the polarization angle ϕ_i increases from 0° to 80°. As the incident angle θ_i increases from 0° to 80° in Fig. 11(b) the real part Re(n) values of the retrieved effective refraction index are also independent of incident angle. However, two different trends can be noticed for the transmission response of the metamaterial (not shown here). For example, in the former case the transmission resonance peaks progressively shrink with the increase of ϕ_i, whereas in the latter the peak slightly shifts upward towards a high frequency with θ_i increasing. But, at any rate, these effects have a limited influence on the real part Re(n) value of the negative refractive index due to broadband performance of metamaterial as shown in Fig. 11. Therefore, these results further confirm that this metamaterial is dependent of the incident angle and polarization angle of the incident field.

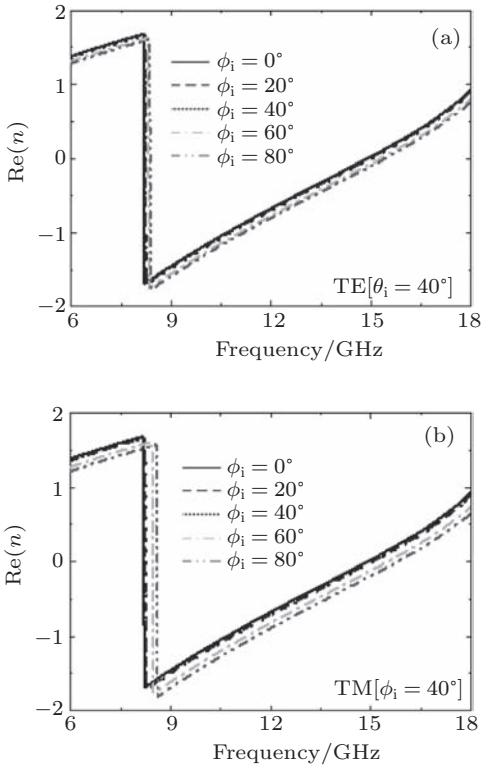


Fig. 11. Curves for Re(n) of retrieved effective refractive index n versus frequency for an obliquely incident TE or TM plane wave at different (a) incident and (b) polarization angles.

From the above analyses, we can conclude that no matter what (normally or obliquely) incident TE or TM mode plane wave is used, the proposed metamaterial is independent of its incident angle and polarization angle. These results are due mainly to the high symmetry of the unit cell, thus the proposed metamaterial can provide an an isotropic response to any linearly polarized incident wave, which is demonstrated in the previous result,[29] where a slight variation of the symmetrical design can have a significant influence on the effective parameters of the metamaterial.

5. Conclusion

A 3D NRI metamaterial with broadband and isotropy is successfully characterized for applications of superlenses in this paper using the CST Microwave Studio 2006. The proposed metamaterial is composed of a periodic array of tightly coupled metallic cross-pairs printed on the six sides of a cube, whose characters consist in high symmetry and superposition of metallic cross-pairs. The field distributions demonstrate that the magnetic and the electric resonances are realized by the coupling between adjacent metallic cross-pairs. The retrieved constitutive parameters,

the coupling field distributions, and the wedge prism experiment show that the metamaterial exhibits an NRI region, whose absolute bandwidth and relative bandwidth can attain up to 6.52 GHz and 56.7%, respectively. In addditon, the insensitivity to arbitrarily (normally or obliquely) incident EM wave with varying incident angle and polarization angle demonstrates that this metamaterial is isotropic. Therefore, the proposed metamaterial is a better candidate material as 3D broadband isotropic NRI metamaterial than the traditional SRR and wire or fishnet structures.

References

[1] Veselago V G 1968 *Sov. Phys. Usp.* **10** 509

[2] Zhang F L, Gaillot D P, Croenne C, Lheurette E, Melique X and Lipppens D 2008 *Appl. Phys. Lett.* **94** 083140

[3] Sellier A, Burokur S N, Kate B and Lustrac A D 2009 *Opt. Express* **17** 6301

[4] Burokur S N, Sellier A, Kante B and Lustrac A D 2009 *Appl. Phys. Lett.* **94** 201111

[5] Smith D R, Padilla W J, Vier D C, Nemat-Nasser S C and Schultz S 2000 *Phys. Rev. Lett.* **84** 4184

[6] Machac J, Rytir M, Protiva P and Zehentner J 2008 *Proc. 38*th *European Microwave Conference* October 28–31, 2008, Amsterdam, Netherlands, p. 547

[7] Chen C H, Qu S B, Xu Z, Wang J F, Ma H and Zhou H 2011 *Acta Phys. Sin.* **60** 024101 (in Chinese)

[8] Chen C H, Qu S B, Wang J F, Ma H, Wang X H and Xu Z 2011 *Chin. Phys.* B **20** 034101

[9] Silveirinha M and Fernandes C A 2005 *IEEE Trans. Microw. Theory Tech.* **53** 1418

[10] Gong B Y, Zhou X and Zhao X P 2011 *Acta Phys. Sin.* **60** 044101 (in Chinese)

[11] Grbic A and Eleftheriades G V 2005 *J. Appl. Phys.* **98** 043106

[12] Zedler M, Caloz C and Russer P 2007 *IEEE Trans. Microwave Theory Tech.* **55** 2930

[13] Koschny T, Zhang L and Soukoulis C M 2005 *Phys. Rev.* B **71** 121103

[14] Wang J F, Qu S B, Xu Z, Fu Z T, Ma H and Yang Y M 2009 *J. Phys.* D: *Appl. Phys.* **42** 155413

[15] Vier D C, Schultz S, Greegor R B, Parazzoli C G, Nielsen J A and Tanielian M H 2009 *IET Microwave Antennas Propag.* **3** 723

[16] Wang B N, Zhou J F, Koschny T and Soukoulis C M 2009 *Appl. Phys. Lett.* **94** 151112

[17] Sanada A 2009 *IEICE Electronics Express* **6** 689

[18] Vendik I B, Odit M A and Kozlow D S 2009 *Metamatrials* **3** 140

[19] Rudolph S M and Gric A 2010 *IEEE Antennas and Propagation Society International Symposium* July 11–17, 2010, Toronto, Ontario, Canada, p. 241

[20] Li T, Liu H, Wang F M, Dong Z G, Zhu S N and Zhang X 2006 *Opt. Express* **14** 11155

[21] Eleftheriades G V 2007 *IEEE Microwave Wireless Components Lett.* **17** 412

[22] Rudolph S M and Gric A 2009 *IEEE International Microwave Symposium* June 7–12, 2009 Boston, Massachusetts, USA, p. 153

[23] Wang J F, Qu S B and Xu Z, Zhang J Q, Ma H, Yang Y M and Gu C 2009 *Photonics and Nanostructures-Fundamentals and Applications* **7** 108

[24] Ma Y G, Wang X C and Ong C K 2008 *Phys. Rev.* E **78** 016605

[25] Smith D R, Vier D C, Koschny T and Soukoulis C M 2005 *Phys. Rev.* E **71** 036617

[26] Chen X, Grzegoczyk T M, Wu B I, Pacheco J and Kong J A 2004 *Phys. Rev.* E **70** 016608

[27] Shelby R A and Smith D R 2001 *Science* **292** 77

[28] Dong Z, Zhu S, Liu H, Zhu J and Cao W 2005 *Phys. Rev.* E **72** 016607

[29] Imhof C and Zengerle R 2007 *Opt. Commun.* **280** 213